BIOCELL
2021 45(1): 49-56

Tech Science Press

miR-21-3p alleviates neuronal apoptosis during cerebral ischemia-reperfusion injury by targeting SMAD2

Fei TIAN*; Gang LIU; Linlin FAN; Zhongyun CHEN; Yan LIANG

Neuro ICU, Neurological Department, Xuanwu Hospital, Capital Medical University, Beijing, 100053, China

Key words: Ischemic stroke, Ischemic reperfusion injury, Neural cells, MicroRNA-21, SMAD2, Apoptosis

Abstract: Cerebral ischemia is due to the formation of blood clots or embolisms in the brain arteries, which leads to local brain tissue necrosis and neural cell apoptosis. Recent studies have shown that microRNA (miRNA) plays an important regulatory role in the pathological process of ischemic injury. The aim of this study is to investigate the role and the mechanism of miR-21-3p and drosophila mothers against decapentaplegic 2 (SMAD2) in cerebral ischemic reperfusion injured (CIRI) neural cells. The CIRI model was established by oxygen-glucose deprivation and recovery process for N2a cells. The cell viability and the apoptotic was evaluated by MTT assay and the Flow Cytometer, respectively. The expression of miR-21-3p and SMAD2 mRNA was detected by real-time fluorescence quantitative PCR (qRT-PCR), and the expression of SMAD2 and apoptotic-related proteins were detected by Western Blotting. Our results showed that miR-21-3p is down-regulated, and SMAD2 is up-regulated in CIRI. Overexpression of miR-21-3p inhibits the apoptosis of neural cells in CIRI. miR-21-3p targets SMAD2 and inhibits SMAD2 expression. Over-expression of SMAD2 eliminates the protective effect of over-expression of miR-21-3p on neural cells in CIRI. Token together, this study provides a theoretical basis for the mechanism of ischemic reperfusion injury in neural cells and a new molecular target for ischemic stroke therapy.

Introduction

Cerebral ischemia is due to the formation of blood clots or embolisms in the brain arteries, which leading to local brain tissue necrosis and neural cells apoptosis (Nagy and Nardai, 2017). However, the restoration of blood flow supply to the brain may further cause reperfusion damage, so-called ischemic reperfusion injury (Lin *et al.*, 2016). The pathogenesis of cerebral ischemic reperfusion injury is complex unclear.

MicroRNA (miRNA) is a class of small RNA that promotes mRNA degradation or inhibits mRNA translation by thereby negatively regulating the expression of target proteins (Fu and Blackshear, 2017). The exact mechanism of neuronal damage during cerebral ischemia is not entirely clear, but recent studies have shown that miRNA plays an important regulatory role in the pathological process of ischemic injury (Wang *et al.*, 2018; Yin *et al.*, 2014). miR-21-3p has been shown to be a powerful anti-apoptotic factor that works through targeting the host's apoptosis gene (Pink *et al.*, 2015). It is expressed in most solid tumor tissues (Hu *et al.*, 2018), while there are few reports of the role of miR-21-3p in neuronal damage caused by ischemic reperfusion injury. The *Drosophila* Mothers Against Decapentaplegic 2 (SMAD2) protein is a key transcriptional regulator in a variety of cell death patterns that control transcription-dependent apoptosis and necrosis procedures in response to a variety of signals, including DNA damage, oxidative stress, and ischemia (Dong *et al.*, 2019). The predicted miR-21-3p target genes were analyzed in a previous study; only three genes (RBPMS, RCBTB1, and ZNF608) were confirmed as miR-21-3p target genes in ovarian cancer cells. RBPMS (RNA-binding protein with multiple splicing) mediates the transcriptional activity of SMAD proteins, mainly by enhancing the phosphorylation of SMAD2 and SMAD3. Upon phosphorylation, SMADs accumulate in the cell nucleus and act as mediators of transcriptional activation (Labibi *et al.*, 2020). N2a cells are mouse-sourced neuroblastoma cells, most of which are neuronal-like and have axon-like structures (Tremblay *et al.*, 2010).

At present, the cell is mainly cultivated in the laboratory as an *in vitro* neuronal cell model and is used to study neuronal cell growth, neurotoxicity, neurodegeneration, and so on.

To sum up, we applied N2a cell lines to explore the role and the mechanism of miR-21-3p and SMAD2 in neural cells

*Address correspondence to: Fei Tian, Email: smile21tian@163.com
Received: 21 August 2020; Accepted: 25 September 2020

Doi: 10.32604/biocell.2021.013794

suffering from cerebral ischemic reperfusion injured (CIRI) and hoped to provide a new molecular target for the treatment of ischemic stroke.

Materials and Methods

Cell culture

N2a cells (ATCC, USA) were cultured in DMEM medium containing 10% fetal bovine serum and cultured in an incubator at 37°C and 5% CO_2. The culture medium was changed every 3 days for subculture. The N2a cells cultured to the logarithmic growth phase were seeded in 6-well plates (1500 μL/well) at 6×10^5 cells/mL. The normal cerebral cortex astrocytes (Control) were obtained as follows: Within 24 h after being harvested, Wistar rat brain cortex was used to disperse the cells by mechanical method and trypsin digestion method to prepare a cell suspension, and inoculate it in a substrate-free culture flask, and cultured in an incubator at 37°C and 5% CO_2.

Neuronal cell ischemic reperfusion injury

When the cell density was appropriate, we replaced the DMEM medium with Earle's balanced salt solution without glucose, transferred the cells to a special incubator for oxygen and sugar deprivation model containing 5% CO_2 and 95% N_2, and incubated them at 37°C for 2 h. Then, the medium was replaced with DMEM medium containing sugar and serum and transferred to a normal CO_2 incubator for 24 h. The above process was used to simulate neuronal ischemia-reperfusion injury.

Cell transfection

GenePharma (Shanghai, China) synthesized miR-21-3p mimics, miR-21-3p inhibitor, SMAD2 plasmid, respective negative controls (NC). According to the manufacturer's instructions, the miR-21-3p mimics (60 nM), miR-21-3p inhibitor (60 nM), SMAD2 plasmid (60 nM), and respective NC were transfected into differentiated podocytes by Lipofectamine 2000 (Invitrogen, Carlsbad, CA, USA). After 2 days of growth, the original medium was discarded, and RPMI-1640 culture medium (Gibco, USA) was selected for the transfected cells.

Cell viability

The conventional MTT assay was used to analyze cell viability. The cells were grown at $2–4 \times 10^4$ cells per well in 96-well microplates. MTT solution (Sigma, USA) was then added to the medium to a final concentration of 0.5 mg/mL and incubated at 37°C for 4 h. Absorbance measurements were read at 450 nm and was calculated. At least three independent repeated experiments were required.

Flow cytometry analysis

The Annexin V-FITC/PI Apoptosis Detection Kit (Becton Dickinson, Rutherford, NJ, USA) was used for the quantification of cellular apoptosis. Briefly, the cells were resuspended in 200 μL annexin binding buffer containing 5 μL PI and 10 μL annexin V-FITC in the dark for 10 min at 25°C. Flow cytometry (Abcam, USA) was used to analyze the double-stained cells. At least three independent repeated experiments were required.

Assessment of reactive oxygen species (ROS) production

Mitochondrial ROS production was evaluated using specific ROS kits (Genmed Scientifics Inc., Wilmington, DE). Mitochondrial fractions (50 μg) were cultured with 6-chloromethyl-2',7'-dichlorodihydro-fluorescein diacetate (CM-H2DCFDA) at 37°C for 15 min. Fluorescence, with excitation and emission wavelengths of 490 and 530 nm, respectively, was monitored by a fluorescence spectrophotometer. At least three independent repeated experiments were required.

Determination of malondialdehyde (MDA) activity

Cells were centrifugated for 15 min at 4500 rpm. The samples were stored at −80°C prior to the analysis of MDA activity, which was evaluated using a commercial ELISA kit (A003-4-4, Nanjing Built Bio, Nanjing, China). At least three independent repeated experiments were required.

Determination of mitochondrial membrane potential (MMP)

MMP was evaluated by using a specific MMP kit (Beyotime, Haimen, China) that included JC-1 (5,5',6,6'-tetrachloro-1,1',3,3'-tetraethyl-imida carbocyanine iodide, C2006, Biyuntian, Shanghai, China), which is a fluorochrome that becomes incorporated into cells depending on the status of the MMP. In this process, staining for reduced JC-1, which emits green fluorescence, indicates a disruption of the mitochondrial inner membrane potential. Briefly, cells in 6-well plates were processed as described in previous experiments, washed with PBS, and cultured with the JC-1 solution at 37°C for 20 min in the dark. The cells were then washed twice with PBS and resuspended in PBS (500 μL). Fluorescence was evaluated by a BD FACSAria II flow cytometer system (BD, Franklin Lakes, NJ). The results are shown in terms of the proportion of cells with a low MMP. At least three independent repeated experiments were required.

Quantitative Real Time-PCR

The total cells RNA was extracted by Trizol reagent (Invitrogen, Carlsbad, CA), and the SuperScript RT kit from Invitrogen (Invitrogen, Carlsbad, CA) was used for reverse transcription. The PowerUp™ SYBR® Green Master Mix (Thermo Fisher Scientific, USA) and the ABI PRISM7900 Sequence Detection System (Applied Biosystems, USA) were used. The $2^{-\Delta\Delta Ct}$ method was used for miRNA and mRNA expression analyses; glyceraldehyde 3-phosphate dehydrogenase (GAPDH) and U6 snRNAs served as the positive controls. At least three independent repeated experiments were required.

Luciferase reporter assay

The mutant (MUT) SMAD2 3'-untranslated region (UTR) and wild-type (WT) SMAD2 3'-UTR, which both contained a putative binding site of miR-21-3p, were synthesized and inserted into the reporter vector of pmirGLO dual-luciferase (YouBio, Changsha, China). Reporter vectors containing the MUT and WT SMAD2 3'-UTRs, and the NC-mimics/miR-206 mimics, were co-transfected into HEK293T cells and cultured until the cells reached 80% confluency. After 48 h, the assay of the dual-luciferase system (Promega, Madison, USA) was used to evaluate the levels of luciferase, which

were normalized to those of the *Renilla* luciferase. At least three independent repeated experiments were required.

Western blotting analysis

Cells were homogenized on ice for half an hour in RIPA buffer (Sigma-Aldrich, USA) with protease inhibitors. The homogenate was then centrifuged at 12000 rpm for 15 min, and the supernatant was collected and stored at −20°C. Electrophoresis on 12% sodium dodecyl sulfate-polyacrylamide gels using Tris-glycine running buffer was performed to separate total proteins, which were then immobilized onto PVDM (Sigma-Aldrich, USA). Nonspecific binding was blocked by gentle shaking in Tris-buffered saline with 3% bovine serum albumin and 0.1% Tween-20 for 1 h at room temperature. Then the membranes were cultured with the following primary antibodies: anti- Bax, Bcl2, caspase 3, caspase 9, cytochrome c (Cyto c) (1:2000, Applygen), anti-SMAD2 (1:1000, Santa Cruz, USA) and anti-GAPDH (1:1000, Applygen), overnight at 4°C. Proteins were visualized by a LAS-4000 mini system (Fujifilm, Japan) and quantified by Quantity One software. Protein expression levels were standardized to those of GAPDH. At least three independent repeated experiments were required.

Statistical analysis

GraphPad 8.0 software was used to analyze the data. Results were presented as mean ± standard deviation (SD), and all experiments were repeated three times. $p < 0.05$ was considered statistically significant, ANOVA was performed to determine the significance of differences among experimental groups.

Results

miR-21-3p is down-regulated in vitro, *and SMAD2 is up-regulated in simulated cerebral ischemia reperfusion model*

An *in vitro* simulated cerebral ischemia-reperfusion injury model was established, we detected the expression of miR-21-3p and SMAD2. As shown in Fig. 1A, qRT-PCR detected the expression levels of miR-21-3p and SMAD2 in the Control group, *in vitro* CIRI group, and found that miR-21-3p was lowly expressed in the CIRI group, while the SMAD2 expression was increased in the CIRI group. Moreover, the results of western blot showed that the protein expression of SMAD2 was markedly increased in the CIRI group, as compared to the control group (Fig. 1B).

Overexpression of miR-21-3p inhibits the apoptosis of neural cells in CIRI

We used 60 nmol/L miR-21-3p mimics and NC mimics plasmids to transfect the modeled cells N2a. As shown in Fig. 2A, the cell viability in the CIRI was markedly decreased as compared with the control group ($p < 0.001$). In contrast, overexpression of the miR-21-3p group demonstrated higher cell viability than the CIRI and CIRI +miR-NC group ($p < 0.05$). Next, we applied flow cytometry to determine the number of apoptotic cells. As demonstrated in Fig. 2B, the cellular apoptosis was markedly increased in the CIRI group as compared to the control group. However, the numbers of apoptosis cells were significantly lower in the CIRI+miR-21-3p mimics group. To further clarify how miR-21-3p protected against mitochondrial pathway apoptosis induced by CIRI, we detected ROS, MDA, MMP, and mitochondrial pathway apoptosis-related proteins in the Control, CIRI, CIRI+miR-NC, and CIRI+miR-21-3p mimics groups. ROS assays showed that the ROS content of the CIRI treatment group was significantly higher than that of the control group ($p < 0.001$). The ROS contents in the CIRI+miR-21-3p were significantly lower than those in the CIRI treatment group ($p < 0.01$, Fig. 2C). The results of the MDA content assays were like those of the ROS assays (Fig. 2D). In addition, a decrease in the MMP became obvious in the CIRI treatment group. These effects were reversed by the administration of miR-21-3p mimics (Fig. 2E). To further clarify how miR-21-3p inhibited mitochondrial pathway apoptosis, we used Western blot analysis to measure the expressions of Cyto c, caspase 9, caspase 3, Bax, and Bcl-2. As illustrated in Fig. 2F, the results from the Western–blot analysis showed a decrease in the Bcl-2 expression level and an increase in the Cyto c, caspase 9, caspase 3, and Bax expression levels in the CIRI treatment group compared with the control group (all $p < 0.01$). These effects were further ameliorated by the administration of miR-21-3p mimics.

miR-21-3p targets SMAD2 and inhibits SMAD2 expression

TargetScan website predicted miR-21-3p target the gene of SMAD2 as shown in Fig. 3A. Fig. 3B showed that WT SMAD2 3'-UTR luciferase activity was inhibited when miR-21-3p mimics were co-transfected with the vector ($p < 0.01$),

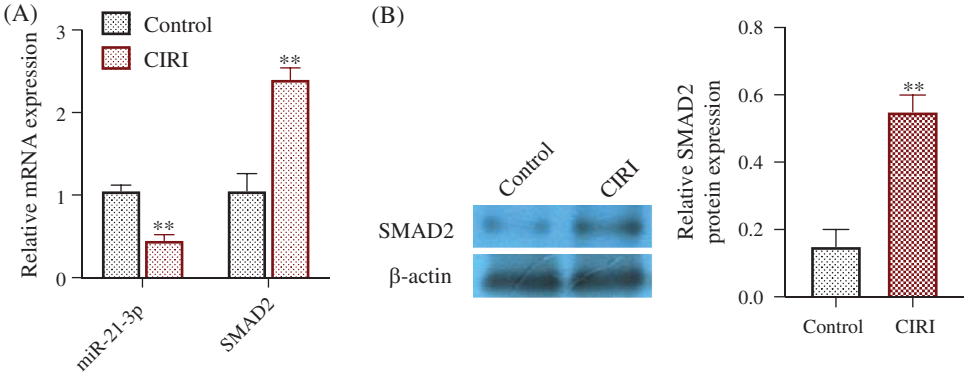

FIGURE 1. miR-21-3p is down-regulated and SMAD2 is up-regulated in simulated cerebral ischemia.
(A) The miR-21-3p and SMAD2 mRNA expression was evaluated by qRT-PCR in Control and CIRI group. (B) The SMAD2 protein expression was evaluated by western blot in Control and CIRI group. **$p < 0.01$ *vs.* Control group.

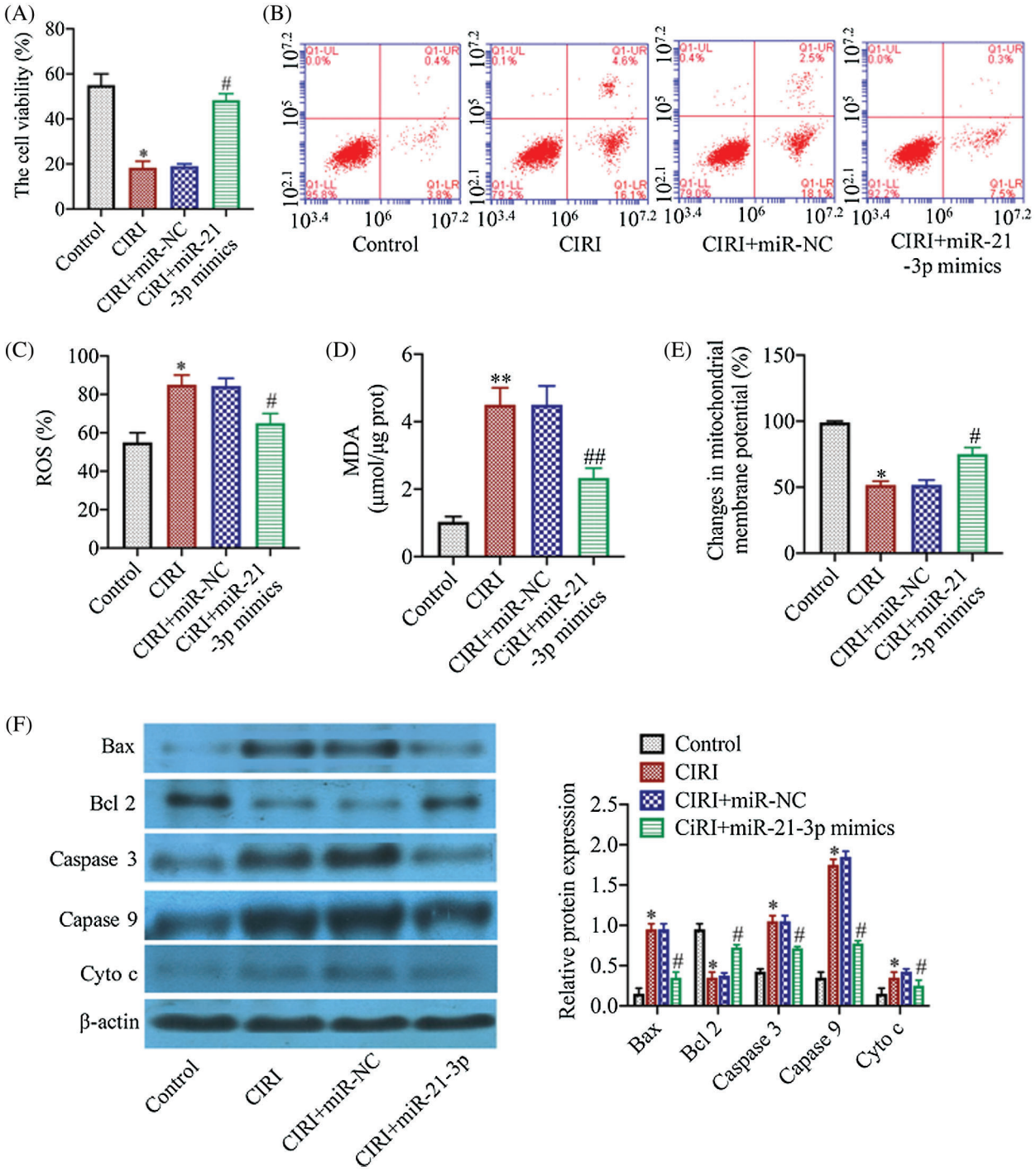

FIGURE 2. Overexpression of miR-21-3p inhibits the apoptosis of nerve cells in CIRI.
(A) The cell viability was evaluated by MTT assay in Control, CIRI, CIRI+miR-NC, and CIRI+miR-21-3p mimics group. (B) The apoptosis of cells was evaluated by flow cytometry in Control, CIRI, CIRI+miR-NC, and CIRI+miR-21-3p mimics group. (C) The ROS production was evaluated using specific ROS kits in Control, CIRI, CIRI+miR-NC, and CIRI+miR-21-3p mimics group. (D) The MDA content was evaluated by ELISA kit. (E) The MMP was evaluated by using a specific MMP kit in Control, CIRI, CIRI+miR-NC, and CIRI+miR-21-3p mimics group. (F) The Bax, Bcl 2, Cyto c, caspase 3 and caspase 9 protein expressions were evaluated by western blot in Control, CIRI, CIRI+miR-NC, and CIRI+miR-21-3p mimics group. $^{*}p < 0.05$, $^{**}p < 0.01$ *vs.* Control group, $^{\#}p < 0.05$, $^{\#\#}p < 0.01$ *vs.* CIRI+miR-NC group.

whereas WT SMAD2 3'-UTR luciferase activity was significantly increased by co-transfection of miR-21-3p inhibitors. After transfection of miR-21-3p mimics and inhibitors into HEK293 cells, the SMAD2 mRNA expression in both cell lines after transfection with miR-21-3p mimics was obviously decreased, while the mRNA expression of SMAD2 was markedly increased after knockdown of miR-21-3p (Fig. 3C). Similar trends were observed in the protein expression of SMAD2 in both cell lines (Fig. 3D).

Over-expression of SMAD2 eliminates the protective effect of over-expression of miR-21-3p on neural cells in CIRI

Results of MTT assay showed that the cell viability of CIRI +miR-21-3p mimics group was inhibited by overexpression

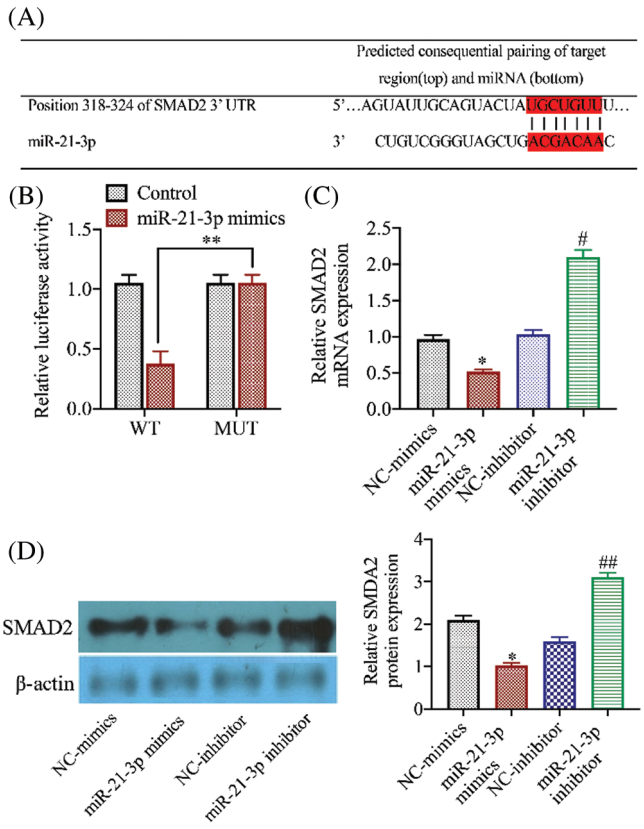

FIGURE 3. miR-21-3p targets SMAD2 and inhibits SMAD2 expression.
(A) TargetScan predicts miR-21-3p and SMAD2 binding sites. (B) Luciferase activity analysis of the targeted relationship of miR-21-3p and SMAD2 in HEK-293T cells in Control and miR-21-3p mimics group. (C) The SMAD2 mRNA expression was evaluated by qRT-PCR in NC-mimics, miR-21-3p mimics, NC inhibitor, and miR-21-3p inhibitor group. (D) The SMAD2 protein expression was evaluated by western blot in NC-mimics, miR-21-3p mimics, NC inhibitor, and miR-21-3p inhibitor group. $^{*}p < 0.05$, $^{**}p < 0.01$ *vs.* Control group, $^{\#\#}p < 0.01$ *vs.* NC inhibitor.

of SMAD2 ($p < 0.05$) (Fig. 4A). At the same time, flow cytometry was performed to detect the cell apoptosis of each group, the cell apoptosis of the CIRI+miR-21-3p mimics group was markedly increased by overexpression of SMAD2 ($p < 0.01$) (Fig. 4B). In addition, results in Figs. 4C and 4D showed that the ROS and MDA levels of the CIRI+miR-21-3p mimics group were blocked through overexpression of SMAD2 ($p < 0.05$, $p < 0.01$), whereas the MMP of the CIRI +miR-21-3p mimics group were dramatically increased after transfection of overexpression of SMAD2 ($p < 0.01$) (Fig. 4E). As illustrated in Fig. 4F, the results from the Western blotting analysis showed the Bcl-2 expression level of CIRI+miR-21-3p mimics group was markedly decreased and the Cyto c, caspase 9, caspase 3, and Bax expression levels of CIRI+miR-21-3p mimics group were markedly increased by overexpression of SMAD2 ($p < 0.01$) (Fig. 4F).

Discussion

The present study investigated the correlation between miR-21-3p and SMAD2 in CIRI model was simulated by N2a cells. It showed that miR-21-3p is down-regulated, and SMAD2 is up-regulated in CIRI. Overexpression of miR-21-3p inhibits the apoptosis of neural cells in CIRI. miR-21-3p targets SMAD2 and inhibits SMAD2 expression. Over-expression of SMAD2 eliminates the protective effect of over-expression of miR-21-3p on neural cells in CIRI.

Compared with other tissues in the body, the brain is more prone to ischemic damage, about 80% of stroke patients are ischemic stroke, and unlike other tissues of the immediate ischemic damage, transient brain ischemia (about 10 min) can produce neuronal damage (Yan *et al.*, 2016). After cerebral ischemia, as oxygen and glucose gradually run out, the energy dependence process necessary for cells is hampered, triggering a series of biological processes, followed by the death of a large number of cells due to necrosis apoptosis or the joint action of both (Puyal *et al.*, 2013). In recent years, there has been growing evidence that non-coding RNA may be involved in stroke, providing new ideas for the study of pathophysiology in stroke (Gabory *et al.*, 2010; Salta and De Strooper, 2012). Cheng and other studies have found that expression miR-21-3p can reduce apoptosis in oxidative stress damage in myocardial cells (Cheng and Zhang, 2010). In addition, miR-21-3p specifically increased expression in myocardial fibroblasts in the area of intracardial injury after myocardial infarction, and the change played an improved effect on the injury (Thum, 2014). For ischemic stroke, miR-21-3p is a strong anti-apoptosis and survival factor, which can reduce the expression of apoptosis-related proteins (Yan *et al.*, 2017). Buller and others found that overexpression of miR-21-3p in *in vitro* cultured cortical neurons significantly inhibited hypoxic hypoxia-induced apoptosis, while inhibition of endogenous miR-21-3p expression aggravated cell death after hypoxia (Deng *et al.*, 2019). In our present study, miR-21-3p was found to be reduced in N2a cells after the treatment of the oxygen-sugar deprivation model, combined with previous studies suggest that miR-21-3p may play a protective role in ischemic neuronal damage. Han *et al.* reported that miR-21-3p could reduce the number of TUNEL-positive neurons, while miR-21-3p reduced the expression level of PTEN, significantly increased the phosphorylation of AKT, and in the neurons transfected miR-21-3p, Bcl-2 expression was enhanced, while caspase 3,

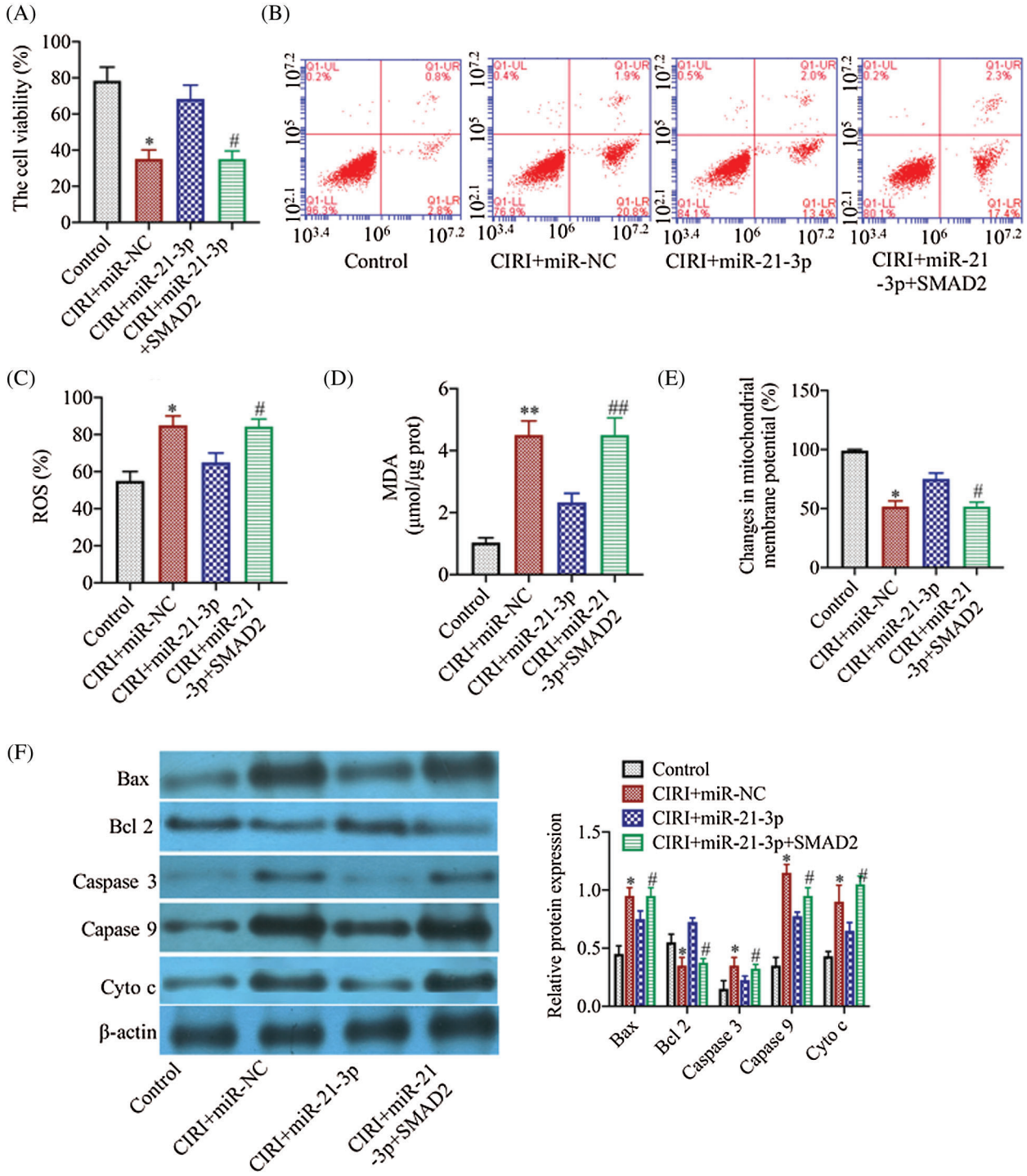

FIGURE 4. Over-expression of SMAD2 eliminates the protective effect of over-expression of miR-21-3p on neural cells in CIRI. (A) The cell viability was evaluated by MTT assay in Control, CIRI+miR-NC, CIRI+miR-21-3p, and CIRI+miR-21-3p+SMAD2. (B) The apoptosis of cells was evaluated by flow cytometry in Control, CIRI+miR-NC, CIRI+miR-21-3p, and CIRI+miR-21-3p+SMAD2. (C) The ROS production was evaluated using specific ROS kits in Control, CIRI+miR-NC, CIRI+miR-21-3p, and CIRI+miR-21-3p+SMAD2. (D) The MDA content was evaluated by ELISA kit. (E) The MMP was evaluated by using a specific MMP kit in Control, CIRI+miR-NC, CIRI+miR-21-3p, and CIRI+miR-21-3p+SMAD2. (F) The Bax, Bcl 2, Cyto c, caspase 3 and caspase 9 protein expressions were evaluated by western blot in Control, CIRI+miR-NC, CIRI+miR-21-3p, and CIRI+miR-21-3p+SMAD2. $^{*}p < 0.05$, $^{**}p < 0.01$ *vs.* Control group, $^{\#}p < 0.05$, $^{\#\#}p < 0.01$ *vs.* CIRI+miR-21-3p group.

caspase 9, and Bax expression were reduced, so miR-21-3p could be activated by PTEN-Akt signal (Han *et al.*, 2014). Lowering downstream apoptosis-related protein expression plays a role in reducing neuroma apoptosis (Mou *et al.*, 2019). In our present study, N2a cells were treated with an oxygen-sugar deprivation model, and the model of hypoxia ischemic injury of *in vitro* nerve cells was set, and overexpression of miR-21-3p also inhibits the apoptosis of neural cells in CIRI.

SMAD2 protein is a key transcriptional regulatory factor in a variety of cell death signaling pathways. Lin *et al.* (2010)

reported that SMAD2's DNA binding domain is mediated by ischemic neuron necrosis and apoptosis by directly binding to death-related protein kinase 1 (Lin *et al*., 2010). In the nucleus, SMAD2 induces expression of pre-apoptosis genes such as Bax, while in the in-line granulocytic matrix, SMAD2 triggers necrosis by interacting with procyclin D (Nabbouh, 2016). In this study, both SMAD2 mRNA and protein were expressed in N2a cells treated with oxygen sugar deprivation, suggesting that SMAD2 may have been involved in ischemic damage to N2a cells.

miRNA inhibits its target gene by binding to 3'UTRs of mRNA. It has been reported that some miRNAs are involved in the SMAD2 pathway, or are regulated by SMAD2, or directly inhibit the expression of SMAD2 or its downstream proteins, indicating the importance of miRNA in the SMAD2 signaling pathway (Hermeking, 2012; Nabbouh, 2016). In a variety of tumor cells, there is a negative correlation in the expression of SMAD2 and miR-21-3p expression (Chau *et al*., 2012; Hu *et al*., 2018). Studies have shown that miR-21-3p inhibits the expression of multiple genes in the SMAD2 pathway. In the current study, miR-21-3p targets SMAD2 and inhibits the expression of SMAD2. In breast cancer cells, inhibiting the expression of miR-21-3p induces the expression of multiple genes regulated by SMAD2 (Báez-Vega *et al*., 2016). miR-21-3p is reduced in glioblastoma cells, activating the p63 and SMAD2 pathways, leading to cell cycle blocking and promote apoptosis (Yang *et al*., 2017). Our study showed that over-expression of SMAD2 eliminates the protective effect of over-expression miR-21-3p on *in vitro* simulated brain ischemic reperfusion damage, suggesting that inhibition of SMAD2 expression by miR-21-3p plays a role in the ischemic reperfusion damage of neural cells.

Conclusion

In summary, in *in vitro* cultured neural cells, miR-21-3p overexpression has a protective effect for ischemic reperfusion injury. This effect may be related to its negative regulation on SMAD2 expression. This study provides a theoretical basis for the mechanism of ischemic reperfusion injury in neural cells and a new molecular target for ischemic stroke therapy.

Availability of Data and Material: All the data supporting these findings is contained within this manuscript.

Funding Statement: The author received no specific funding for this study.

Conflicts of Interest: The authors declare that they have no conflicts of interest to report regarding the present study.

References

Báez-Vega PM, Vargas IME, Valiyeva F, Encarnación-Rosado J, Roman A, Flores J, Marcos-Martínez MJ, Vivas-Mejía PE (2016). Targeting miR-21-3p inhibits proliferation and invasion of ovarian cancer cells. *Oncotarget* **7**: 36321–36337. DOI 10.18632/oncotarget.9216.

Chau B N, Xin C, Hartner J, Ren S, Castano A P, Linn G, Li J, Tran P T, Kaimal V, Huang X, Chang A N, Li S, Kalra A, Grafals M, Portilla D, MacKenna D A, Orkin S H, Duffield J S (2012). MicroRNA-21 promotes fibrosis of the kidney by silencing metabolic pathways. *Science Translational Medicine* **4**: 121ra18. DOI 10.1126/scitranslmed.3003205.

Cheng Y, Zhang C (2010). MicroRNA-21 in cardiovascular disease. *Journal of Cardiovascular Translational Research* **3**: 251–255. DOI 10.1007/s12265-010-9169-7.

Deng Y, Chen D, Gao F, Lv H, Zhang G, Sun X, Liu L, Mo D, Ma N, Song L, Huo X, Yan T, Zhang J, Miao Z (2019). Exosomes derived from microRNA-138-5p-overexpressing bone marrow-derived mesenchymal stem cells confer neuroprotection to astrocytes following ischemic stroke via inhibition of LCN2. *Journal of Biological Engineering* **13**: 34. DOI 10.1186/s13036-019-0193-0.

Dong Z, Sun Y, Wei G, Li S, Zhao Z (2019). Ergosterol ameliorates diabetic nephropathy by attenuating mesangial cell proliferation and extracellular matrix deposition via the TGF-β1/Smad2 signaling pathway. *Nutrients* **11**: 483. DOI 10.3390/nu11020483.

Fu M, Blackshear PJ (2017). RNA-binding proteins in immune regulation: A focus on CCCH zinc finger proteins. *Nature Reviews Immunology* **17**: 130–143. DOI 10.1038/nri.2016.129.

Gabory A, Jammes H, Dandolo L (2010). The H19 locus: Role of an imprinted non-coding RNA in growth and development. *BioEssays* **32**: 473–480. DOI 10.1002/bies.200900170.

Han Z, Chen F, Ge X, Tan J, Lei P, Zhang J (2014). miR-21 alleviated apoptosis of cortical neurons through promoting PTEN-Akt signaling pathway *in vitro* after experimental traumatic brain injury. *Brain Research* **1582**: 12–20. DOI 10.1016/j.brainres.2014.07.045.

Hermeking H (2012). MicroRNAs in the p53 network: micromanagement of tumour suppression. *Nature Reviews Cancer* **12**: 613–626. DOI 10.1038/nrc3318.

Hu Y, Rao SS, Wang ZX, Cao J, Tan YJ, Luo J, Li HM, Zhang WS, Chen CY, Xie H (2018). Exosomes from human umbilical cord blood accelerate cutaneous wound healing through miR-21-3p-mediated promotion of angiogenesis and fibroblast function. *Theranostics* **8**: 169–184. DOI 10.7150/thno.21234.

Labibi B, Bashkurov M, Wrana JL, Attisano L (2020). Modelling the control of TGFβ/Smad nuclear accumulation by the Hippo pathway effectors, Taz/Yap. *iScience*, **23**(8): 101416.

Lin L, Wang X, Yu Z (2016). Ischemia-reperfusion injury in the brain: mechanisms and potential therapeutic strategies. *Biochemistry & Pharmacology* **5**: 1–16.

Lin Y, Hupp TR, Stevens C (2010). Death-associated protein kinase (DAPK) and signal transduction: additional roles beyond cell death. *FEBS Journal* **277**: 48–57. DOI 10.1111/j.1742-4658.2009.07411.x.

Mou Z, Wang Y, Li Y (2019). Brazilein induces apoptosis and G1/G0 phase cell cycle arrest by up-regulation of miR-133a in human vestibular schwannoma cells. *Experimental and Molecular Pathology* **107**: 95–101. DOI 10.1016/j.yexmp.2018.12.010.

Nabbouh A (2016). Effect of Imiquimod and derivatives compounds EAPB0203 and EAPB0503 on Leukemia/lymphoma models. *PLoS One* **12**: 182022–182032.

Nagy Z, Nardai S (2017). Cerebral ischemia/repefusion injury: From bench space to bedside. *Brain Research Bulletin* **134**: 30–37. DOI 10.1016/j.brainresbull.2017.06.011.

Pink RC, Samuel P, Massa D, Caley DP, Brooks SA, Carter DRF (2015). The passenger strand, miR-21-3p, plays a role in mediating

cisplatin resistance in ovarian cancer cells. *Gynecologic Oncology* **137**: 143–151. DOI 10.1016/j.ygyno.2014.12.042.

Puyal J, Ginet V, Clarke PGH (2013). Multiple interacting cell death mechanisms in the mediation of excitotoxicity and ischemic brain damage: a challenge for neuroprotection. *Progress in Neurobiology* **105**: 24–48. DOI 10.1016/j.pneurobio.2013.03.002.

Salta E, De Strooper B (2012). Non-coding RNAs with essential roles in neurodegenerative disorders. *Lancet Neurology* **11**: 189–200. DOI 10.1016/S1474-4422(11)70286-1.

Thum T (2014). Noncoding RNAs and myocardial fibrosis. *Nature Reviews Cardiology* **11**: 655–663. DOI 10.1038/nrcardio.2014.125.

Tremblay RG, Sikorska M, Sandhu JK, Lanthier P, Ribecco-Lutkiewicz M, Bani-Yaghoub M (2010). Differentiation of mouse Neuro 2A cells into dopamine neurons. *Journal of Neuroscience Methods* **186**: 60–67. DOI 10.1016/j.jneumeth.2009.11.004.

Wang P, Shao BZ, Deng Z, Chen S, Yue Z, Miao CY (2018). Autophagy in ischemic stroke. *Progress in Neurobiology* **163-164**: 98–117. DOI 10.1016/j.pneurobio.2018.01.001.

Yan H, Rao J, Yuan J, Gao L, Huang W, Zhao L, Ren J (2017). Long non-coding RNA MEG3 functions as a competing endogenous RNA to regulate ischemic neuronal death by targeting miR-21/PDCD4 signaling pathway. *Cell Death & Disease* **8**: 1775. DOI 10.1038/s41419-017-0047-y.

Yan H, Yuan J, Gao L, Rao J, Hu J (2016). Long noncoding RNA MEG3 activation of p53 mediates ischemic neuronal death in stroke. *Neuroscience* **337**: 191–199. DOI 10.1016/j.neuroscience.2016.09.017.

Yang F, Luo L, Zhu ZD, Zhou X, Wang Y, Xue J, Zhang J, Cai X, Chen ZL, Ma Q, Chen Y-F, Wang YJ, Luo YY, Liu P, Zhao L (2017). Chlorogenic acid inhibits liver fibrosis by blocking the miR-21-regulated TGF-β1/Smad7 signaling pathway *in vitro* and *in vivo*. *Frontiers in Pharmacology* **8**: 350. DOI 10.3389/fphar.2017.00929.

Yin KJ, Hamblin M, Chen YE (2014). Non-coding RNAs in cerebral endothelial pathophysiology: emerging roles in stroke. *Neurochemistry International* **77**: 9–16. DOI 10.1016/j.neuint.2014.03.013.